

# **Hail Detection with Polarimetric Radar: A Review**

Report Prepared for the Federal Aviation Administration  
30 September 2004

EDWARD A. BRANDES

Research Applications Program  
National Center for Atmospheric Research

AND

ALEXANDER V. RYZHKOV

Cooperative Institute for Mesoscale Meteorological Studies, University of Oklahoma  
and  
National Severe Storms Laboratory

## **1. Introduction**

Dual-polarization radars typically transmit horizontally and vertically polarized waves and receive polarized backscattered signals. Because illuminated hydrometeors are not spherical, their radar backscatter cross sections are not the same for the two polarizations. The electromagnetic waves are subject to scatter, differential attenuation, differential phase shifts, and depolarization. Changes in returned signals yield information regarding particle size, shape, orientation, and thermodynamic phase. Because hailstones are typically larger than raindrops, hail dominates radar power measurements. Algorithms to detect hail with polarimetric measurements rely on the departure of measurements from the "rain-only" case (Leitao and Watson 1984; Aydin et al. 1986; Balakrishnan and Zrnić 1990a; Smyth et al. 1999). The location of the hail can be precisely specified. Importantly, the suite of polarimetric measurements provides some redundancy that can be useful for eliminating false alarms.

While information regarding hail size and rates can be obtained, these activities are not treated explicitly in this report. Readers are referred to studies of Ulbrich and Atlas (1982), Balakrishnan and Zrnić (1990b), and Husson and Pointin (1989). Polarimetric measurements obtained in the upper regions of thunderstorms may be useful for "predicting" subsequent surface hail, but such capabilities are yet to be explored.

In this review the impact of hail on polarimetric measurements is discussed and illustrated with examples. Several proposed detection techniques using combinations of polarimetric variables are then examined, applied to two hail storms, and their potential for operational use is evaluated.

## **2. Polarimetric measurements**

Polarimetric measurements with strong hail signatures include radar reflectivity ( $Z$ ),

differential reflectivity ( $Z_{DR}$ ), linear depolarization ratio ( $LDR$ ), co-polar correlation coefficient ( $\rho_{HV}$ ), and differential propagation phase ( $\Phi_{DP}$ ). [For detailed descriptions of these parameters, their usage, and typical values for different hydrometeor types, see Doviak and Zrnić (1993, Chapter 8). Additional discussion of polarimetric hail signatures is given by Bringi et al. (1984), Illingworth et al. (1986), Aydin et al. (1986), Zrnić et al. (1993), and Smyth et al. (1999).] The radar reflectivity factor at horizontal ( $H$ ) and vertical polarization ( $V$ ) for a unit volume is

$$Z_{H,V} = \frac{\lambda^4}{\pi^5 |K_w|^2} \int_0^{D_{\max}} \sigma_{H,V}(D) N(D) dD \quad ,$$

where  $\lambda$  is the radar wavelength (mm),  $K_w$  is the dielectric factor for water,  $\sigma_{H,V}(D)$  are the particle radar backscattering cross sections at horizontal and vertical polarization ( $\text{mm}^2$ ),  $N(D)$  is the particle distribution ( $\text{mm}^{-1} \text{m}^{-3}$ ), and  $D$  is the particle equivalent volume diameter (mm). Reflectivity is generally computed in units of  $\text{mm}^6 \text{m}^{-3}$  but expressed in dBZ ( $10 \times \log Z_H$ ). Hailstones are typically much larger than raindrops; and consequently, they have strong impact on radar reflectivity. The likelihood of hail increases as reflectivity increases.

Differential reflectivity ( $Z_{DR}$ , in dB) is defined (Seliga and Bringi 1976) as

$$Z_{DR} = 10 \times \log(Z_H / Z_V)$$

with  $Z_H$  and  $Z_V$  in linear units. Attenuation in severe thunderstorms can impact  $Z_H$  and  $Z_{DR}$ . Consequently, part adjustments for attenuation have been made based on differential propagation phase measurements (Ryzhkov and Zrnić 1994).

Differential reflectivity is positive (negative) for particles whose major axes are close to horizontal (vertical) in the mean. Raindrops tend to flatten and orient themselves with their major axes close to horizontal, giving  $Z_{DR}$  values typically between 0.3 to 3 dB. Larger values are possible for drop-size distributions (DSDs) dominated by large drops as often seen at the leading edge of convection. Hailstones tend to tumble as they fall creating a random distribution of orientations;  $Z_H$  and  $Z_V$  become similar in magnitude causing  $Z_{DR}$  to be small ( $< 0.5$  dB).

The utility of reflectivity and differential reflectivity for distinguishing between rain and hail was demonstrated by Bringi et al. (1984) and Leitaó and Watson (1984). For example, in the Bringi et al. study, rain was characterized by low to moderate radar reflectivity (mostly  $< 45$  dBZ) and  $Z_{DR}$  as large as 4 dB. Hail associated with radar reflectivity  $> 55$  dBZ and  $Z_{DR}$  values near 0 dB. The presence of hail causes a negative correlation between  $Z_H$  and  $Z_{DR}$  and large  $Z_{DR}$  gradients. With large hail  $Z_{DR}$  may be  $< 0$  dB (Bringi et al. 1984; Lipschutz et al. 1986; Zrnić et al. 1993; Ryzhkov and Zrnić 1994). The implication is that large hail may fall with its major axes oriented vertically (Knight and Knight 1970). However, different resonant effects that occur at the two polarizations as hail size increases (Battan 1973, Fig. 10.7; Seliga and Bringi 1978) could cause a negative value even for an oblate hailstone based on size–radar wavelength considerations alone.

Aspherical hydrometeors whose principal axes are not aligned with the electrical field of the transmitted energy cause a small amount of the energy to be depolarized and appear in the orthogonal direction. The linear depolarization ratio ( $LDR$ , in dB) is defined as the logarithm of the ratio of cross-polar and co-polar signals

$$LDR = 10 \times \log(Z_{VH} / Z_H) \quad ;$$

$Z_{VH}$  is the signal received at vertical polarization (cross-polar return) for a transmitted horizontally-polarized wave. Measurements for rain and dry snow are small, on the order of  $-34$  to  $-25$  dB (depending on antenna isolation). Signatures are strongest for large wetted ice particles characteristic of melting layers. For hail,  $LDR$  is positively correlated with radar reflectivity and can be  $> -15$  dB. Large  $LDR$  values can also arise from ground clutter, range-folded echoes, sidelobes, low signal-to-noise ratios, and leakage between the two polarization channels of the radar. The planned upgrade to modify the WSR-88D for polarimetric measurements calls for the simultaneous transmission and reception of horizontally and vertically polarized radiation. This configuration precludes the  $LDR$  measurement.

The co-polar correlation coefficient at zero lag ( $\rho_{HV}$ ) is computed from the reflectivity at horizontal and vertical polarization.<sup>1</sup> This parameter is sensitive to the distribution of particle axis ratios, particularly for mixed-phase hydrometeors and mixtures of hydrometeor types. Theoretical values are  $\sim 0.99$  for raindrops, ice crystals, and dry aggregates. For hail,  $\rho_{HV}$  is typically less than  $0.95$  and can drop below  $0.75$ – $0.85$  for large hail (Ryzhkov and Zrnić 1994).

The above parameters are derived from power measurements that depend upon backscattering properties of illuminated particles. Radar waves are also subject to propagation effects such as attenuation and phase shifts. The differential phase shift ( $\Phi_{DP}$ ) between horizontally and vertically propagating polarized waves at a distance  $r$  is given by

$$\Phi_{DP}(r) = \Phi_0 + \delta(r) + \int_0^r K_{DP}(r) dr \quad ,$$

where  $\Phi_0$  is the radar hardware offset between signals at the two polarizations,  $\delta(r)$  is the backscatter differential phase shift, and  $K_{DP}$  is the two-way specific differential phase due to propagation. For an anisotropic medium like rain or pristine ice crystals, propagation constants for horizontally and vertically polarized waves differ. Horizontally polarized waves “see” a larger particle cross-section and consequently propagate more slowly than vertically polarized waves. Signals returned to the receiver for the two polarizations exhibit different accumulative phase (time) shifts depending on hydrometeor size, shape, orientation, quantity, and distance from the radar; and in the absence of backscatter phase shifts,  $\Phi_{DP}$  normally increases monotonically with range. Hail that tumbles or is near spherical in shape makes little contribution to  $K_{DP}$ . Large oriented hail will have little impact if it is dry because of its small refractive index. However, large wetted oriented hail and snow aggregates in the Mie scattering region can produce a backscatter differential phase shift that often is seen as a temporary decrease in  $\Phi_{DP}$  with range (Zrnić et al. 1993; Smyth et al. 1999).

### 3. Proposed hail detection techniques

---

<sup>1</sup>For radars alternately transmitting electromagnetic energy at horizontal and vertical polarization the correlation coefficient at zero time lag is estimated statistically. Estimated correlations can be greater than 1.0

*a. Reflectivity–differential reflectivity*

A simple polarimetric hail-detection algorithm incorporating reflectivity and differential reflectivity measurements was proposed by Leitao and Watson (1984). They determined a “rain-only” area in  $Z_H$ – $Z_{DR}$  space for radar measurements obtained in England. Storm events with low freezing levels and strong convection were excluded. A boundary,  $f(Z_{DR})$  in dB, which defined the limits of the rain distribution was

$$\begin{aligned} f(Z_{DR}) &= -4 Z_{DR}^2 + 19 Z_{DR} + 37.5 \text{ dB} & 0 < Z_{DR} < 2.5 \text{ dB} \\ &= 60 \text{ dB} \quad . & 2.5 \leq Z_{DR} < 4.0 \text{ dB} \end{aligned} \quad (1)$$

Following the work of Leitao and Watson, Aydin et al. (1986) defined a hail differential reflectivity parameter ( $H_{DR}$ ) given by

$$H_{DR} = Z_H - g(Z_{DR}) \quad , \quad (2)$$

where

$$\begin{aligned} g(Z_{DR}) &= 27 \text{ dB} & Z_{DR} \leq 0 \text{ dB} \\ &= 19 * Z_{DR} + 27 \text{ dB} & 0 \leq Z_{DR} \leq 1.74 \text{ dB} \\ &= 60 \text{ dB} & Z_{DR} > 1.74 \text{ dB} \quad . \end{aligned} \quad (3)$$

The units of  $Z_H$  and  $Z_{DR}$  are dBZ and dB, respectively. The segmented line [ $g(Z_{DR})$ ] was determined with disdrometer observations from rainstorms in Illinois and Colorado. The lower bound for  $g(Z_{DR})$  (27 dB) is designed to prevent false hail designations at reflectivity values where hail is not likely. Relation (3) is intended to allow for  $Z_H$  and  $Z_{DR}$  measurement errors and drop oscillations. Raindrop shapes were assumed to respond to surface tension and hydrostatic pressure as given by Green (1975). A positive value of  $H_{DR}$  indicates hail. Hail likelihood and size tend to increase with the magnitude of  $H_{DR}$  (Aydin et al. 1986; Brandes and Vivekanandan 1998).

For illustration we examine measurements from a rapidly evolving complex of severe hailstorms observed in the Oklahoma panhandle with NCAR’s S-Pol radar (Fig. 1). This storm, which produced  $\frac{3}{4}$  inch (19 mm) hail, was selected because of its isolation, proximity to the radar, well-defined developmental stages, and occurrence of several issues related to hail detection. Hail was first detected about 15 min after first echo detection at that elevation. Figures 2a–4a show a time sequence of differential reflectivity measurements plotted against radar reflectivity. The measurements have been averaged over five range bins in linear space (a distance of 0.75 km) and are from 1.2° antenna elevation for the region shown in Fig. 1. Measurements prior to hailfall (0036 UTC), when hail was first observed (0041 UTC), and after hail ended (0115 UTC) are presented.

Measurements from 0036 UTC (Fig. 2a) reveal a maximum reflectivity of 56 dBZ. Associated differential reflectivity values were roughly 4 dB, indicative of very large drop median volume diameters ( $D_{0s}$ ). We suspect that large drops supported by small hail cores or small partly-melted hail with a horizontal torus of water about their midsections were not present because large hail would likely reach the 1.2° level before such hydrometeors. An extrapolation with the  $D_0$ – $Z_{DR}$  relation of Brandes et al. (2004) suggests that maximum  $D_{0s}$  may have exceeded

13 June 2002  
0041 UTC  
1.2 Degree Elevation Angle

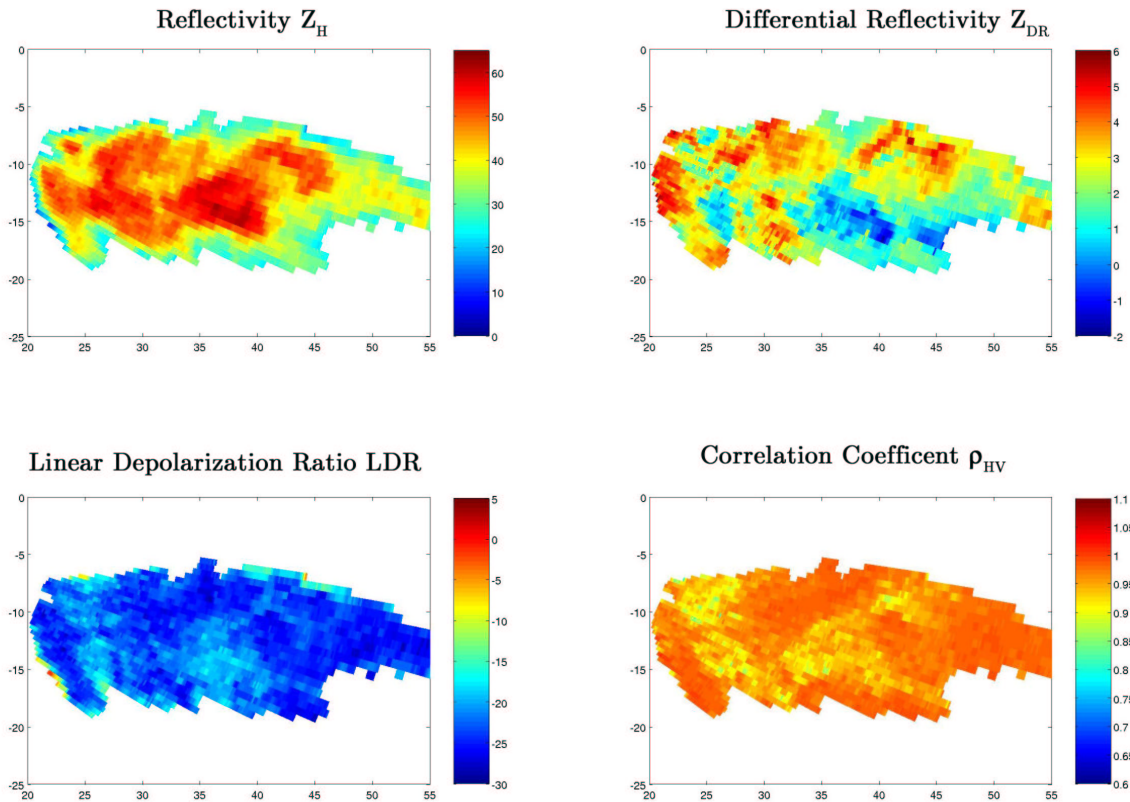


*FIG. 1: Polarimetric radar measurements obtained in a severe hailstorm observed in Oklahoma. North is toward the top of the figure.*

5 mm. The  $D_0$  indicated for a differential reflectivity value of 2 dB, a minimum value for a reflectivity of about 40 dBZ, is 2.1 mm. The distribution of data points shows considerable scatter which is attributed to DSD variations associated with strong updrafts and drop size sorting by the storm flow.

The hail discriminating boundaries (1) and (3) are overlaid in Figs. 2a–4a. Measurements thought to be contaminated by hail lie below and to the right of the curves. At 0036 UTC all  $Z_H$ – $Z_{DR}$  measurement pairs lie in the rain-only region and well above both discriminating boundaries. Strong indications of hail were present when the storm was next sampled (0041 UTC, Fig. 3a). Figure 1 shows the spatial distribution of reflectivity, differential reflectivity, linear depolarization ratio, and correlation coefficient for this storm stage. The spatial

13 June 2002, 0036 UTC

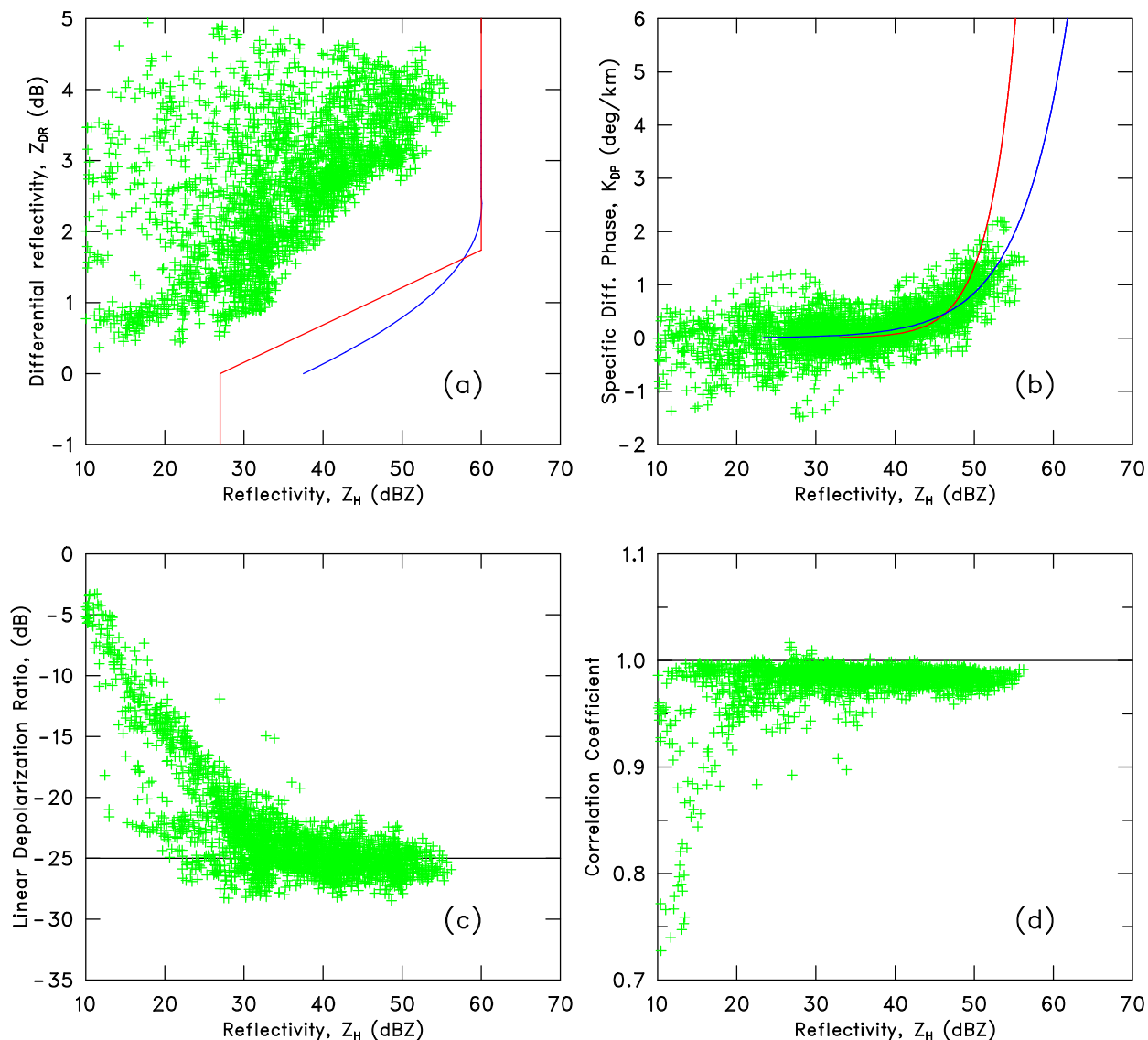


FIG. 2: Differential reflectivity (a), specific differential phase (b), linear depolarization ratio (c), and cross-correlation coefficient (d) plotted against radar reflectivity for a severe hailstorm observed in Oklahoma on 13 June 2002 at 0036 UTC. Overlaid curves are explained in the text.

distribution of  $H_{DR}$  at 0041 UTC is given in Fig. 5.

Data points to the right of the curves (Fig. 3a) result from the inverse relationship between  $Z_H$  and  $Z_{DR}$  that occurs when hail is present, whereby hail increases  $Z_H$  because of its size but reduces  $Z_{DR}$  because it tumbles. Data pairs with high reflectivity and small  $Z_{DR}$  (e.g., near  $Z_H = 60$  dBZ and  $Z_{DR} = 0$  dB) are clearly hail affected and correctly designated by both algorithms. Points displaced farthest from the boundaries probably associate with the largest hail. Measurement pairs having a reflectivity of 55 dBZ and a differential reflectivity of 2–2.5 dB are also likely contaminated by hail because they depart from the rain-only case (Fig. 2a).

13 June 2002, 0041 UTC

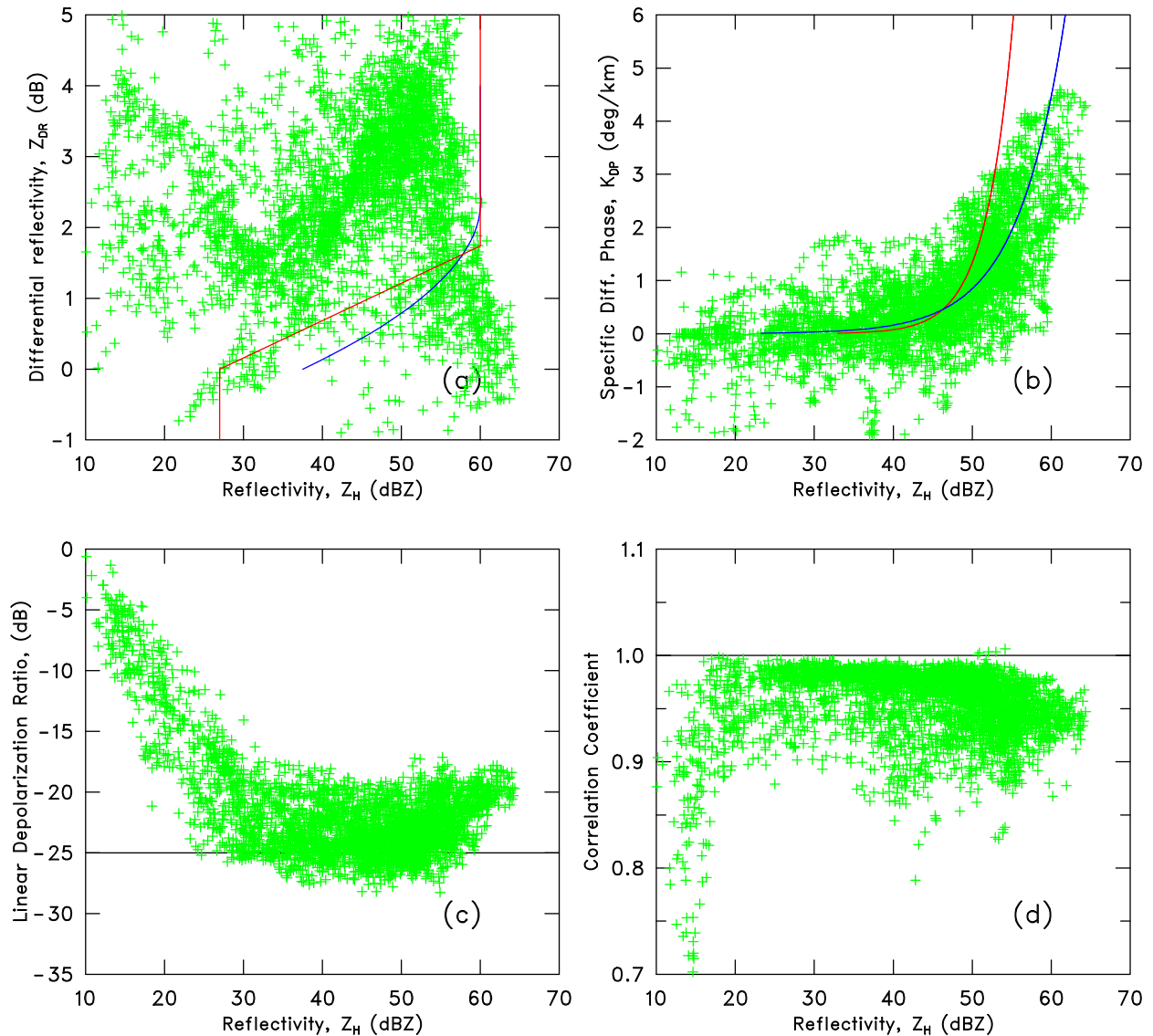


FIG. 3: As in Fig. 2, except for 0041 UTC.

These data points illustrate the principal problem with boundaries like that of Leitao and Watson and Aydin et al. Data pairs along the boundaries are the limits of rain-only measurements and not typical values. They represent the smallest median volume diameters for a particular reflectivity value, whereas hailstorms are often characterized by populations of large drops. Regardless, the 13 June storm shows that hail-contaminated measurements can exist well above the boundaries. The region between the distribution of  $Z_H$ - $Z_{DR}$  pairs at 0036 UTC and the boundaries (1) and (3) represents a "gray area" in hail detection. All detection schemes which incorporate these two measurements will be affected.

Some data points with intermediate reflectivity 40–50 dBZ and  $Z_{DR} < 1$  dB are probably influenced by sidelobe contamination and would have resulted in false alarms. Data points with

13 June 2002, 0115 UTC

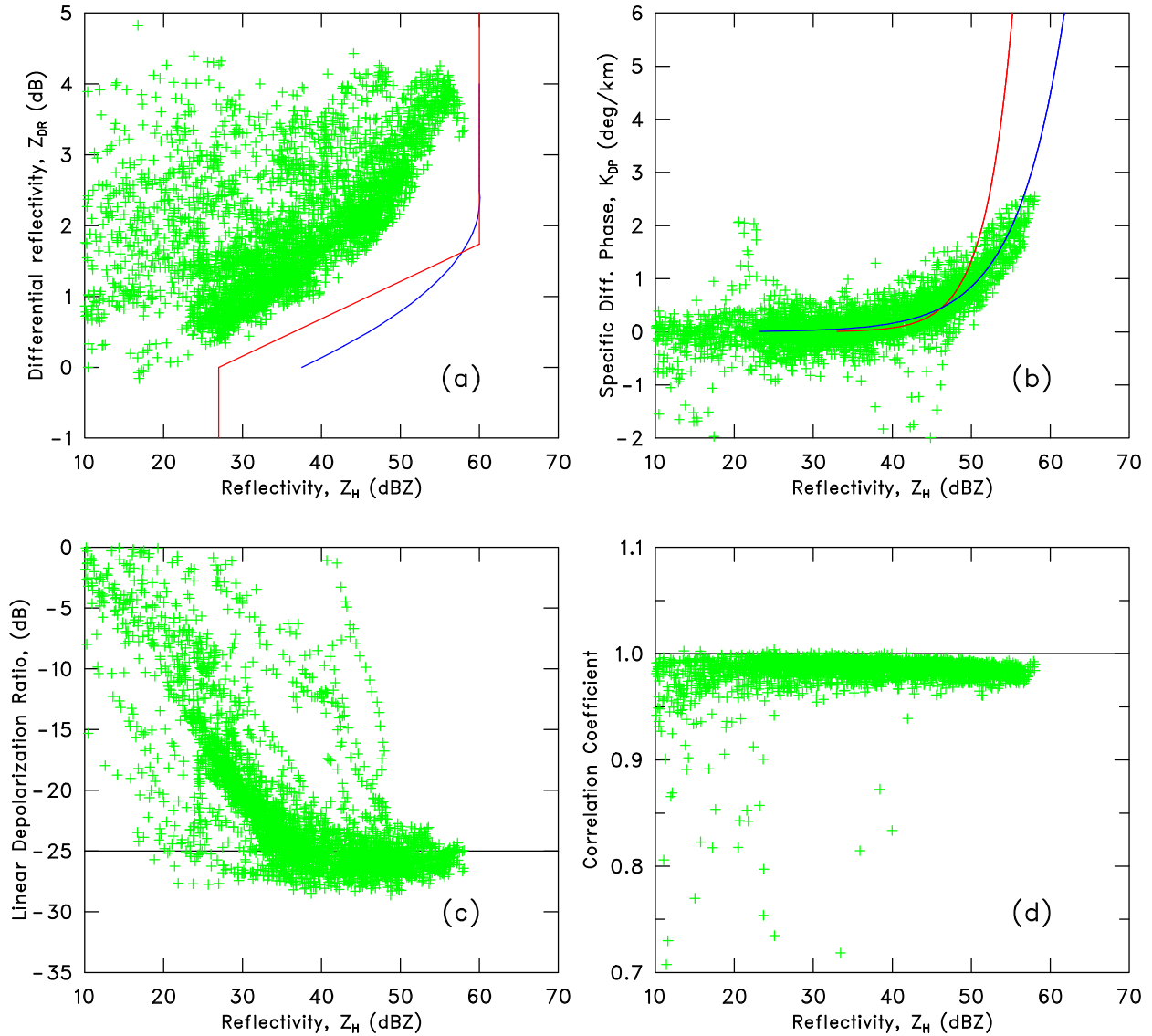


FIG. 4: As in Fig. 2, except for 0115 UTC.

$Z_H$  of  $\sim 30$  dBZ and  $Z_{DR} = 0$  dB reside at the far side of the storm and are caused by uncompensated differential attenuation (Figs. 1 and 5;  $x = 44$  to  $49$  km,  $y = -18$  to  $-15$  km). A number of false detections with the algorithm of Aydin et al. result. Raising the minimum value for  $g(Z_{DR})$  would help in this regard. Compared to algorithms discussed below, the designated hail region (Fig. 5) is relatively small. This is due to the presence of large drops and hail-contaminated measurements with negative  $H_{DRS}$ .

Aydin et al. recognized potential bias problems with their hail detection approach and note that hail shafts are marked with gradients of  $H_{DR}$ . An alternate procedure may be to compute local gradients of  $H_{DR}$ . However, computed gradients would be influenced by imposed thresholds that set  $g(Z_{DR})$  to fixed values for small and large  $Z_{DR}$  (Fig. 6). Also, some storms

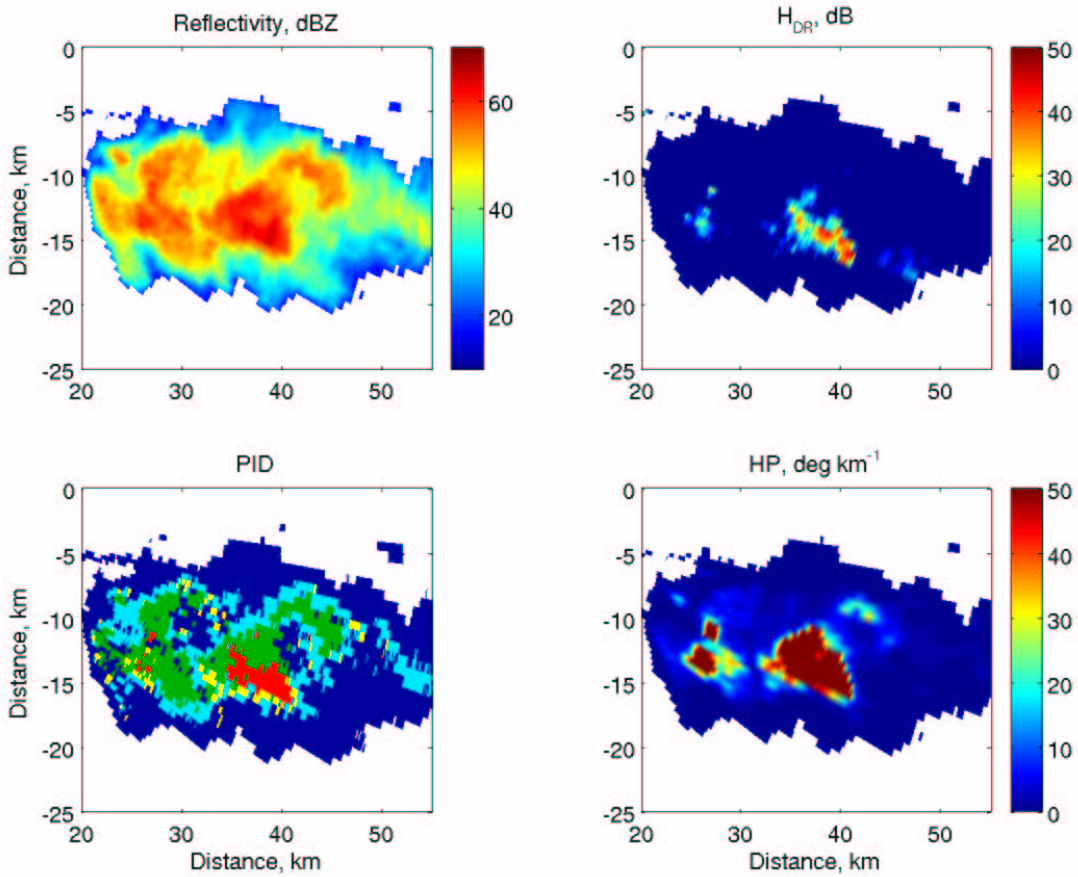


FIG. 5: Radar reflectivity (slightly smoothed) and hail designations made with potential algorithms for the dataset in Fig. 1. PID classifications are for hail (red) and hydrometeor mixtures: graupel–hail (yellow), rain–hail (green), and graupel–rain (light blue).

may contain hail that falls with its major axis close to horizontal. Smyth et al. (1999) describe what were believed to be hail-contaminated measurements with  $Z_{DR}$  of 3–5 dB. Such occurrences would not be detectable with algorithms that assume hail tumbles.

Hail indications ended by 0115 UTC (Fig. 4a). The  $Z_H$ – $Z_{DR}$  distribution again resembled that at 0036 UTC (Fig. 2a) except that minimum  $Z_{DR}$  values had decreased somewhat in response to smaller drop median volume diameters in the declining stage of the storm.

### b. Difference reflectivity

Golestani et al. (1989) propose to detect hail with the difference reflectivity parameter

$$Z_{DP} = 10 \times \log(Z_H - Z_V) \quad ,$$

which is defined only for  $Z_H > Z_V$ . Again, the procedure for hail detection is to determine

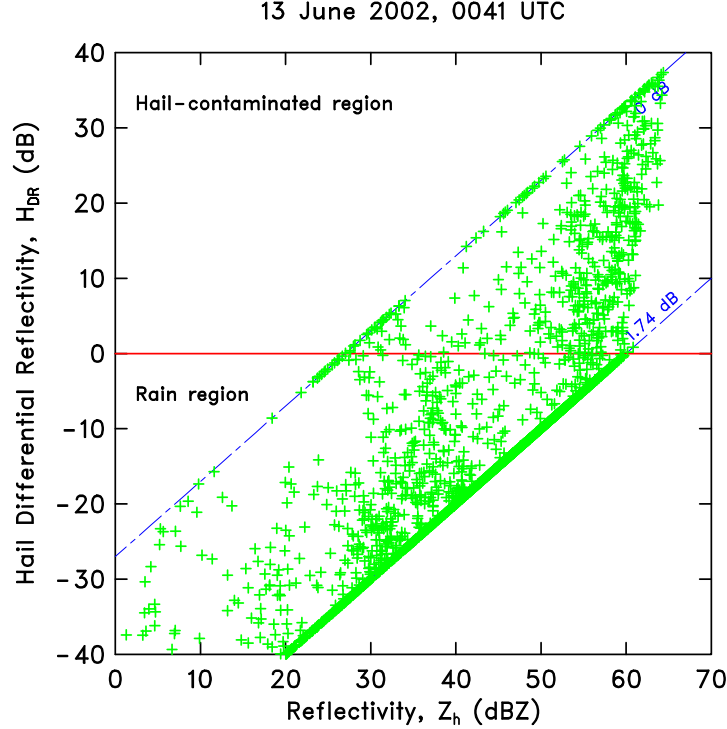


FIG. 6:  $H_{DR}$  plotted versus  $Z_H$  for the hailstorm at 0041 UTC. Designated hail-contaminated (rain) measurements lie above (below) the horizontal line. The limits for the distribution,  $Z_{DR} = 0$  dB [ $g(Z_{DR}) = 27$  dB] and 1.74 dB [ $g(Z_{DR}) = 60$  dB], are shown by dashed lines.

departures from the rain-only case. The distribution of radar reflectivity-difference reflectivity parameter pairs for the pre-hail (rain-only) stage of storm development is plotted in Fig. 7a. A least-squares fit to the observations is

$$Z_{DP} = -6.831 + 1.087 Z_H \quad . \quad (4)$$

Examination reveals a linear relationship with some broadening of the distribution at lower reflectivity due to a higher relative noise level in the measurements. Hail-contaminated measurements will be displaced to the right of and below the rain-only relation. Experience shows that the slope of the line and intercept are sensitive to DSD variations. Smaller drop median volume diameters would associate with smaller  $Z_{DP}$  values.

Application to the hail stage is presented in Fig. 7b. Hail is manifest by significant departures to the right of Eq. (4) causing a relative broadening of the  $Z_H - Z_{DP}$  distribution at high reflectivity. The difference reflectivity shares many attributes with the differential reflectivity. Hail signatures begin approximately at a reflectivity of 50 dBZ. Because  $Z_{DP}$  is undefined for  $Z_H < Z_V$ , a condition often associated with large hail,  $Z_{DP}$  is limited as a hail detection parameter. However,  $Z_{DP}$  has value as a diagnostic tool. Drawing a boundary around a region of a storm suspected to contain hail and plotting  $Z_H - Z_{DP}$  pairs would readily verify the presence of hail if the distribution at high reflectivity is as broad as that in Fig. 7b. The distribution at 0115 UTC is identical to that at 0036 UTC (not shown).

13 June 2002

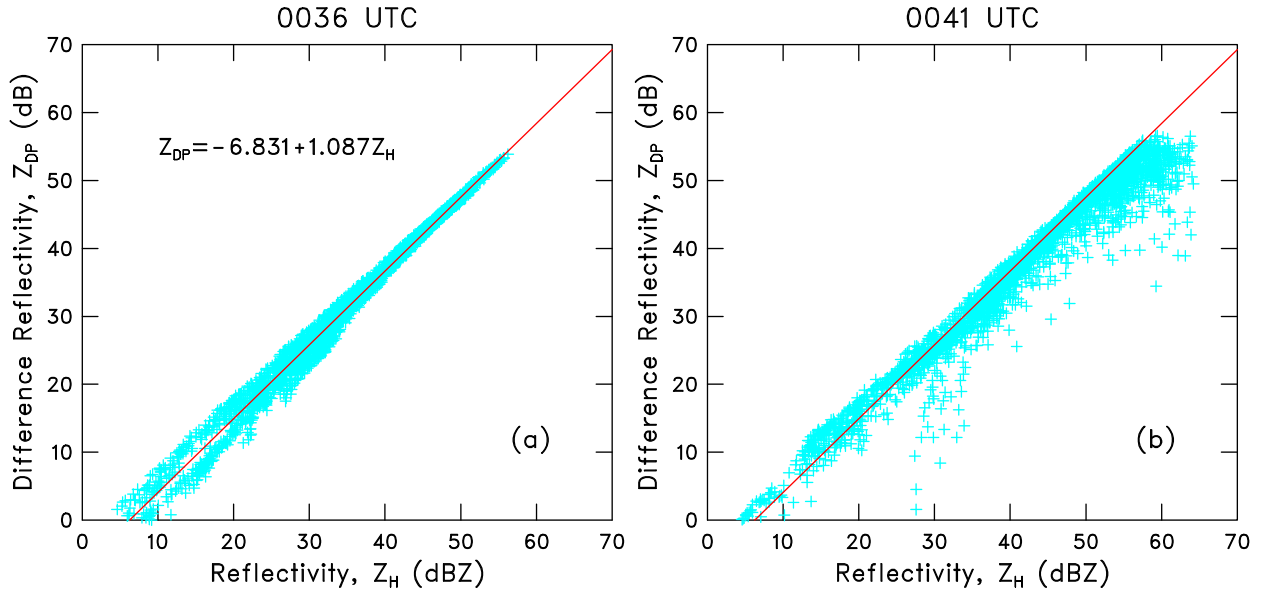


FIG. 7:  $Z_{DP}$  plotted versus  $Z_H$  for the hailstorm at (a) 0036 and (b) 0041 UTC. The red line is a least squares fit [Eq. (4)] for the pre-hail stage (0036 UTC).

c. Differential propagation phase and radar reflectivity

Balakrishnan and Zrnić (1990a) proposed to identify hail with departures in  $Z_H$  and  $K_{DP}$  measurement pairs from the rain-only case. The presence of hail increases  $Z_H$  because of its size; but if the hail tumbles or is dry, it makes negligible contribution to  $K_{DP}$ . From radar measurements Balakrishnan and Zrnić (1990a) determined pure rain and hail-contaminated measurements were separated by

$$Z_H = 8 \log (K_{DP}) + 49.0 \quad , \quad (5)$$

with  $Z_H$  in dB and  $K_{DP}$  in  $\text{deg km}^{-1}$ . This relation is plotted in Figs. 2b–4b (red line). Hail-contaminated data pairs purportedly lie below and to the right of the curve. There is an obvious problem. Parameter pairs for the pre-hail stage (Fig. 2b) are broadly distributed along the discrimination boundary until about 50 dBZ and then deviate in the mean into the hail region to the right of the boundary. The hail stage (Fig. 3b) is characterized by specific differential phase estimates exceeding  $4^\circ \text{ km}^{-1}$ . The largest values are at the highest reflectivity, suggesting that the hail is mixed with heavy rain. Numerous data points lie in the hail region to the right of the red curve. It is doubtful that all these measurements are contaminated by hail. Also, there is no ready separation between rain-only and hail-contaminated measurement pairs as in Fig. 3a. The hail signature is obscured due to a relatively small hail signal. Hail discrimination with the  $K_{DP}$ – $Z_H$  pair was examined by Ryzhkov and Zrnić (1994). Their Fig. 6, which has many of the characteristics seen in Fig. 3b, also shows observations that did not agree very well with Eq. (5).

Part of the problem may lie with the large drops on 13 June which enhance radar reflectivity.

Potential problems with Eq. (5) were recognized by Smyth et al. (1999) who determined that for large  $K_{DP}$  (heavy rain) the predicted  $Z_H$  was too small. Smyth et al. suggest that a better discriminator is

$$Z_H = 13.86 \log(K_{DP}) + 51.0 \quad . \quad (6)$$

This relation is a modification of a pure rain relation given by Balakrishnan and Zrnić (1990a) based on Green's axis ratios and a Marshall-Palmer DSD. Equation (6) is plotted as the blue line in Figs. 2b–4b. The adjusted relation offers some improvement, but a high incidence of false alarms persists for the pre-hail and post hail stages.

A hail parameter based on  $K_{DP}$  and  $Z_H$  can be computed from

$$H_{DP} = Z_{H,m} - Z_{H,c} \quad , \quad (7)$$

where  $Z_{H,m}$  is the radar-measured radar reflectivity and  $Z_{H,c}$  is an estimate of radar reflectivity computed from the radar estimate of  $K_{DP}$  using (5) or (6). The distribution of  $H_{DP}$  [with Eq. (6)] is presented in Fig. 8. The  $H_{DP}$  designations are noisy. Some of the largest values occur with  $Z_H < 50$  dBZ and small  $K_{DP}$  due the fact that (5) and (6) become asymptotic to  $K_{DP} = 0^0 \text{ km}^{-1}$ . The false alarms could be eliminated by setting a lower reflectivity limit for computation purposes. Because many data points in Fig. 3b are distributed along the hail boundaries (5) and (6), much of the storm core region is designated as contaminated by hail (positive values of  $H_{DP}$ ). There are large areas, some with  $Z_H > 50$  dBZ, where  $K_{DP}$  is negative and  $H_{DP}$ , as formulated, can not be computed. These traits make the approach of Balakrishnan and Zrnić (1990a) unattractive for hail determination.

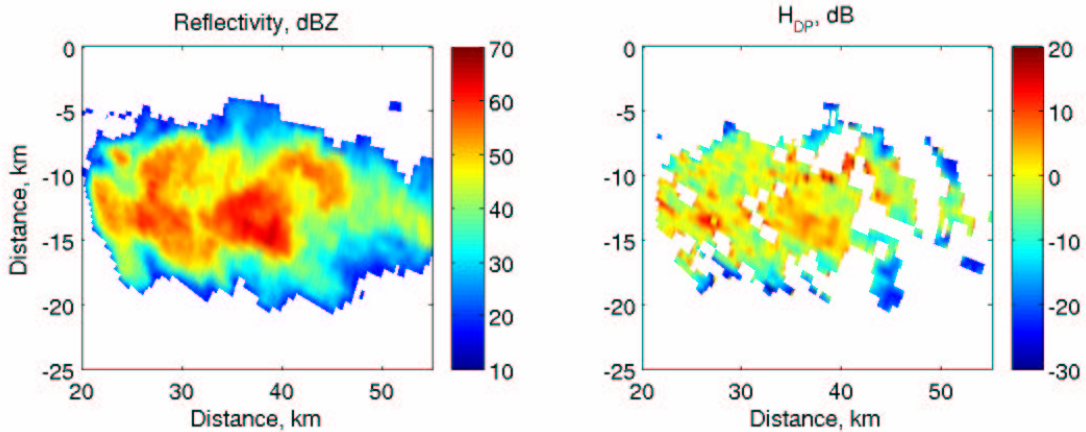


FIG. 8: Distribution of hail designations using the method of Balakrishnan and Zrnić (1990a) as modified by Smyth et al. (1999).

*d. Fuzzy logic approach*

Recognizing that polarimetric signatures for hail are not always unique and overlap those for other hydrometeors, fuzzy logic approaches using the full suite of polarimetric measurements have been proposed (e.g., Vivekanandan et al. 1999). Membership functions are employed to determine the degree to which a particular measurement represents the likelihood of hail. For example, the current membership function for reflectivity for the “hail” category of the real time algorithm that operates on NCAR's S-Pol radar assigns a membership value of “0” for a reflectivity value less than 45 dBZ—essentially indicating that hail is unlikely. The membership value increases linearly to 1 for a reflectivity of 50 dBZ and remains at that value for higher reflectivity values. The membership function increases linearly for intermediate values. Membership values for differential reflectivity are 1 for  $Z_{DR} \leq -1$  dB and 0 for  $Z_{DR} \geq 0.5$  dB. Again, the membership function increases linearly for intermediate values. Member function values for all parameters are similarly obtained. Each radar parameter is then weighed for each hydrometeor classification, and the most likely dominant hydrometeor type selected.

The current NCAR hydrometeor classification algorithm (HCA) attempts to make designations for hail and rain–hail, graupel–hail, and graupel–rain mixtures. Application to the 13 June storm is shown in Fig. 5 (PID panel). A core region of hail (red,  $x = 37$ ,  $y = -16$  km) is flanked by graupel–hail and rain–hail regions. There is also an outer region of graupel–rain. While the designations seem plausible, the total areal coverage of predicted ice forms is thought to be overestimated. Verification of the various hail categories will require a focused effort.

*e. Consistency method*

This method is a variation of that using radar reflectivity and specific differential propagation phase. Consistency among  $Z_H$ ,  $Z_{DR}$ , and  $K_{DP}$  dictates that any two parameters can be used to determine the third parameter (Goddard et al. 1994). For example,  $K_{DP}$  for rain can be estimated from  $Z_H$  and  $Z_{DR}$  with (Vivekanandan et al. 2003)

$$K_{DP} = 6.64 \times 10^{-5} Z_H Z_{DR}^{-2.053} \quad (8)$$

The units for  $Z_H$  and  $Z_{DR}$  are linear. Equation (8) is based on simulations with the constrained-gamma DSD model of Zhang et al. (2001) and raindrop axis ratios of Brandes et al. (2002).

An inconsistency arises between relations like (8) and polarimetric measurements when hail is present (Smyth et al. 1999). A hail parameter ( $HP$ ) can be determined as

$$HP = K_{DP,c} - K_{DP,m} \quad (9)$$

where  $K_{DP,c}$  is the estimated value of  $K_{DP}$  computed with (8) from radial distributions of  $Z_H$  and  $Z_{DR}$ ; and  $K_{DP,m}$  is the estimated specific differential phase computed from measurements of  $\Phi_{DP}$ . Hail will generally increase  $K_{DP,c}$  relative to  $K_{DP,m}$ .  $HP$  should be close to  $0^\circ \text{ km}^{-1}$  for rain. Large positive departures from  $0^\circ \text{ km}^{-1}$ , beyond that expected from statistical error, signify hail.

The spatial distribution of  $HP$  (Fig. 5) essentially predicts hail in the same general location as that determined with the  $H_{DR}$  and fuzzy-logic methods. There is a background region with  $HP < 10^\circ \text{ km}^{-1}$  (light blues) that roughly coincides with the rain–hail region designated with

the fuzzy-logic algorithm. The small  $HP$ s correspond to  $Z_H$ - $Z_{DR}$  measurement pairs that mostly lay between the rain distribution of 0036 UTC and the boundaries (1) and (3). This "gray area" is problematic for all algorithms. In the figure,  $HP$  values are truncated at  $50^\circ \text{ km}^{-1}$ . Maximum values exceed  $350^\circ \text{ km}^{-1}$ . [Expressing  $HP$  in dB would produce a more manageable range of parameter values. But this would pose a problem for  $HP \leq 0^\circ \text{ km}^{-1}$ , a condition most likely to occur at low reflectivity.] Importantly, the magnitude of  $HP$  can be related to the probability of hail and maximum hail size, a property that might be useful.

#### *f. Another hailstorm example*

Polarimetric radar measurement pairs for a hailstorm producing dime-size hail in east-central Florida at 1857 UTC on 5 August 1998 are given in Fig. 9. The displacement of the  $Z_H$ - $Z_{DR}$  distribution close to the hail discrimination boundary of Aydin et al. (panel a) discloses that drop median volume diameters are much smaller for this air mass thunderstorm than for the Oklahoma storm. The scattering of data points centered at  $Z_H = 57$  dBZ and  $Z_{DR} = 1.5$  dB are separated from the general distribution and are probably contaminated by hail. Only some of these points are designated by the algorithms of Leitao and Watson and Aydin et al. as hail. Data points near  $Z_H = 57$  dBZ and  $Z_{DR} = 2.4$  dB are probably contaminated as well but are not readily distinguishable from the rain-only measurements. In addition, there are a number of spurious hail designations with the algorithm of Aydin et al. for reflectivity of 27–57 dBZ. For the most part these associate with drop-size distributions characterized by unusually small drops. Some measurement pairs of  $Z_H$ - $K_{DP}$  associated with high reflectivity are displaced well into the hail region established by Balakrishnan and Zrnić. These measurements confirm the weak hail signal at high reflectivity with the  $H_{DR}$  parameter.

The spatial distribution of hail designations is shown in Fig. 10. A small region of weak  $H_{DR}$  hail signal is located near  $x = -1$  and  $y = 41$  km. The fuzzy logic algorithm designates this region as having a rain-hail mixture (PID panel). The hail parameter ( $HP$ ) has a region of strong signature which matches that of the other algorithms. There is a large surrounding region of background values with  $HP$  as large as  $30^\circ \text{ km}^{-1}$ . It is unlikely that small hail or ice pellets existed over this entire region. Rather, hail is probably confined to the small region defined by high gradients of  $HP$  and large values (red). Inspection of the background values reveals that they associate with moderate to strong reflectivity and small  $Z_{DR}$  (small drops). The implication is that  $HP$  is highly sensitive to DSD variations.

The distribution of  $Z_{DP}$ - $Z_H$  pairs for the Florida storm is shown in Fig. 11. The broad distribution of data points for reflectivity  $> \sim 52$  dBZ signifies hail. The red line is the least squares fit for the Oklahoma storm [Eq. (4)]. Smaller drop sizes with the Florida storm cause a mean displacement of 1–2 dB from that in the Oklahoma storm.

## **4. Examination of $LDR$ and $\rho_{HV}$ fields**

Panels (c) in Figs. 2–4 and 9 show the distribution of  $LDR$ . All panels reveal considerable leakage between the two polarization states for reflectivity less than  $\sim 30$  dBZ. The contamination occurs in storm fringe areas. For the pre-hail stage of the Oklahoma storm (Fig. 2c)  $LDR$  averages  $-25$  dB for the higher reflectivity values. The lack of a positive correlation

5 August 1998, 1857 UTC

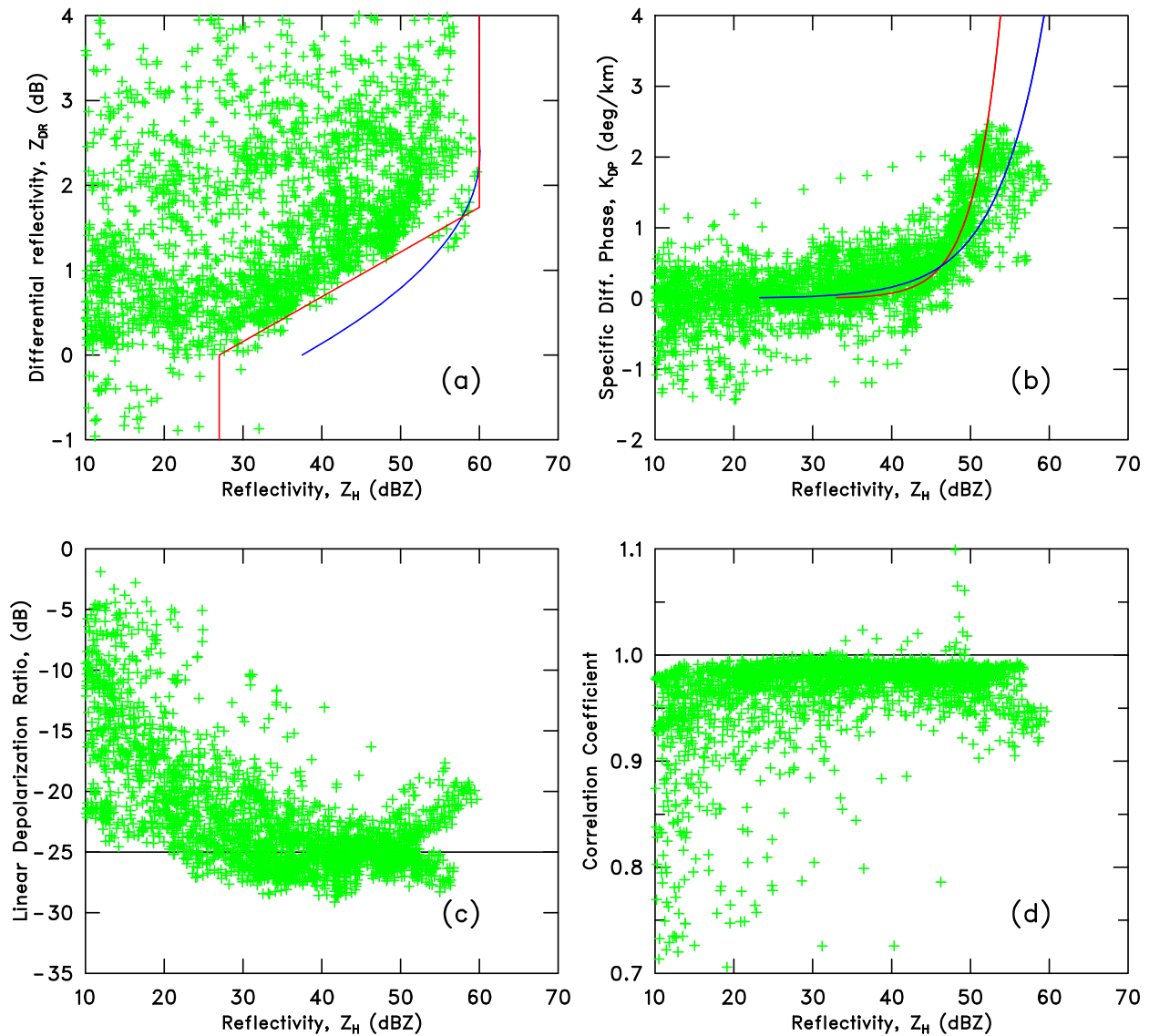


FIG. 9: As in Fig. 2, except at  $0.5^\circ$  antenna elevation for a hailstorm observed in Florida. The relationship between  $LDR$  and  $Z_H$  for large  $Z_H$  is a sign that the measurements are not dominated by hail. The relationship changes at 0041 UTC (Fig. 3c) where for  $Z_H > \sim 50$  dBZ  $LDR$  increases to

approximately  $-20$  dB. Although the signature is well separated from that for rain ( $-25$  dB), the broadened distribution with  $LDR > -20$  dB for a wide range of reflectivity makes it difficult to establish a "hail threshold". The post-hail stage (Fig. 4c) shows a distribution much like the pre-hail stage, except that  $LDR$  is slightly smaller. The distribution of  $LDR$  for the Florida storm (Fig. 9c) reveals a distinct grouping of data points centered near  $Z_H = 55$  dBZ and  $LDR = -22$  dB that are believed to be associated with hail.

Correlation coefficients for the 13 June storm prior to the appearance of hail (Fig. 2d) are

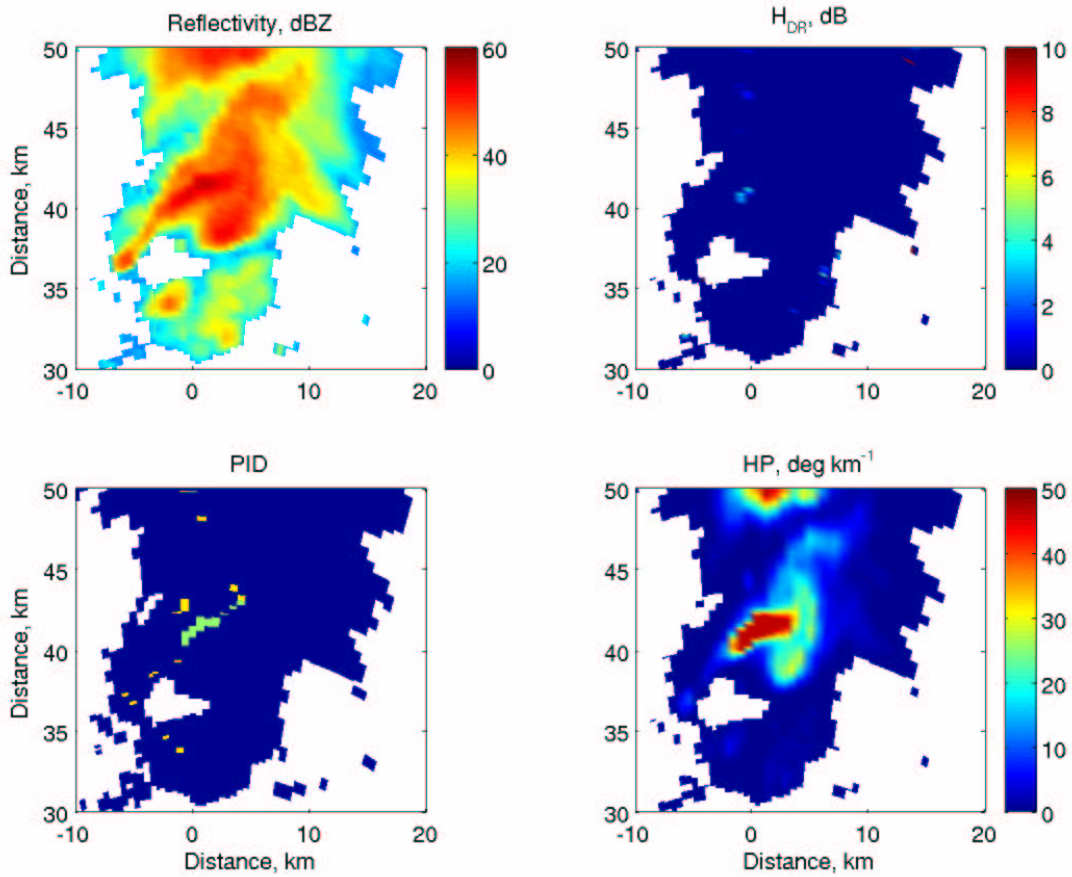


FIG. 10: As in Fig. 5, except for Florida thunderstorm.

slightly smaller than 1.0, averaging 0.98–0.99 for reflectivity  $>35$  dBZ. There is a tendency for  $\rho_{HV}$  to decrease slightly as  $Z_H$  increases. This is thought to be caused by increased oscillations associated with large drops. Low  $\rho_{HV}$  values for  $Z_H < 35$  dBZ are believed to result from ground clutter contamination and signal noise. Reflectivity values associated with hail are paired with reduced  $\rho_{HV}$  measurements that in some cases fall below 0.90 (Fig. 3d). At this stage, maximum correlation coefficients have decreased slightly in the mean and the distribution has widened. Parameter values return to rain-only conditions once the hail ceases (Fig. 4d). For the Florida storm (Fig. 9d) measurements with  $\rho_{HV} = 0.94$  and  $Z_H > \sim 50$  dBZ associate with hail.

Other than for data quality control or with the fuzzy-logic approach where parameter weights are relatively small,  $LDR$  and  $\rho_{HV}$  have been little used for hail detection. Nevertheless, these measurements may be the deciding factor when designations by the described algorithms are ambiguous. In addition to system leakage,  $LDR$  is more susceptible than  $\rho_{HV}$  to contamination by range-folded echoes and low signal-to-noise ratios. A strong negative correlation exists between  $LDR$  and  $\rho_{HV}$  for moderate to strong precipitation. Hence, the loss of  $LDR$  with the planned hardware configuration for polarimetric WSR-88Ds should have little impact on hail detection capabilities and the loss of  $LDR$  should be more than offset by faster scanning times.

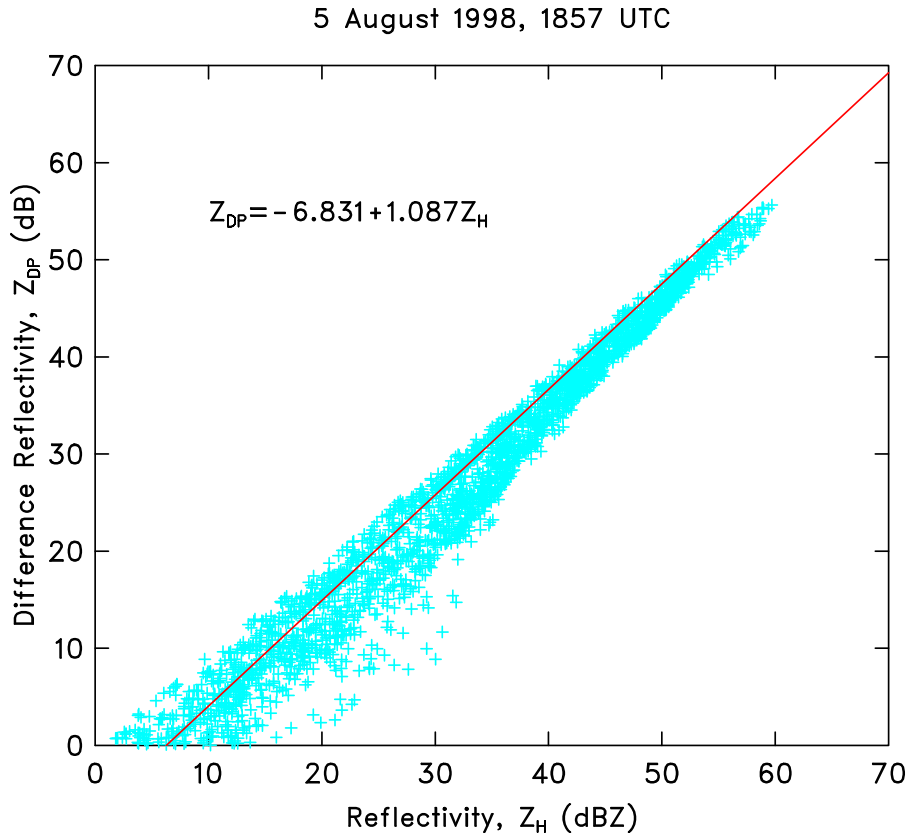


FIG. 11:  $Z_{DP}$  plotted versus  $Z_H$  for the Florida hailstorm at 1857 UTC. The red line is the least squares fit [Eq. (4)] for the pre-hail stage of the Oklahoma storm.

## 5. Verification

An “operational” evaluation of differential reflectivity for hail detection was conducted by Lipschutz et al. (1986). The approach, based on the work of Leito and Watson, determined a probability of detection (POD) of 0.56 compared to a radar reflectivity-based algorithm (the original NEXRAD algorithm) of 0.68. Lipschutz et al. note that many polarimetric algorithm failures were for small hail and attributed the problem to imposed parameter thresholds. In spite of the disappointing results, they conclude that the polarimetric technique had great potential but needed further testing. Husson and Pointin (1989) found a strong negative correlation ( $-0.856$ ) between  $Z_{DR}$  and hail size.

Nanni et al. (2000) evaluated the algorithm of Aydin et al. with a C-band radar. Radar measurements were made at 15 min intervals. Observations from 330 hail pads within 75 km of the radar provided verification. Several analysis constraints were imposed to eliminate issues related to infrequent sampling and attenuation. Hail associated with  $H_{DR} > 13$  dB rather than all positive values. This suggests a bias problem. The probability of detection was 0.9 was determined for radar signatures within 2 km of the hail pads. The critical success index was 0.6, and the false alarm rate was 0.3. Performance may have been influenced by imposed constraints

which eliminated one half of the events. The authors note that many false alarms were close to pads that recorded hail.

An examination of the fuzzy-logic approach to detect hail was conducted by Heinselman and Ryzhkov (2004). The method was compared to the current Hail Detection Algorithm used on the WSR-88D. The polarimetric algorithm outperformed the existing algorithm in overall accuracy and skill. The fuzzy-logic method classified both the absence and occurrence of hail better than random forecasts. For four events there was a 6% increase in the probability of detection, a 31% decrease in the false alarm ratio, and a 30% increase in the critical success ratio. However, situations occurred in which observed hail was not detected.

#### 4. Summary and conclusions

All hail detection techniques discussed here are based on departures from the rain-only case. All methods show some sensitivity to DSD variations. Hence, potential problems are likely to occur with storms characterized by unusually large drops (e.g., the Oklahoma storm) or small drops (the Florida storm). More study of the gray area is needed since measurements in this region will associate with hail in some storms but not in others. Changing algorithm parameters for seasonal or geographical factor to reduce the impact of gray-area measurements will impact algorithm performance parameters such as the critical success index or probability of detection. Hence, the goal is to develop procedures that minimize DSD sensitivity. The difference reflectivity is a step in this direction if the broadness of the distribution at high reflectivity is used as a metric rather than the departure from a predetermined relationship. However, a disadvantage with this method is that the parameter is undefined for  $Z_H \leq Z_V$ .

Cursory evaluation has uncovered problems with the  $Z_H-K_{DP}$  parameter set that stem from a small separation between rain-only and hail-contaminated measurements and a high noise level in  $K_{DP}$ . Solving these issues seems unnecessary due to more robust hail signatures with other hail detection methods. An advantage with the fuzzy-logic detection method is that in marginal hail events additional parameters can be weighed. The fuzzy-logic method gives discrete classifications which some users may find attractive. However, some hail designations are made with higher confidence than others and that information is not currently conveyed. A disadvantage with this approach is that a multitude of thresholds and parameter weights must be specified. The consistency method ( $HP$  index) is also sensitive to DSD variations. This problem may be mitigated somewhat by deriving a relation similar to (8) from observed rather than simulated DSDs. Although a relationship has not been determined, larger  $HP$  values probably associate with greater likelihood of hail and larger size. An advantage with the consistency method is that, other than the selection of Eq. (8), it has no tunable parameters.

Attempts at verification generally show improved results with polarimetric measurements over algorithms based on radar reflectivity alone. Indeed, decreases in false alarm rates and increases in critical success ratios of ~30% are indicated. However, the verification dataset is small. A systematic comparison of the various techniques on a large common dataset obtained from a variety of climatic regimes is required.

*Acknowledgment:* The assistance of NCAR staff Scott Ellis, Benjamin Hendrickson, and Kyoko Ikeda in the construction of Figures 4 and 9 is greatly appreciated.

## REFERENCES

- Aydin, K, T. A. Seliga, and V. Balaji, 1986: Remote sensing of hail with a dual linear polarization radar. *J. Climate and Appl. Meteor.*, **25**, 1475–1484.
- Balakrishnan, N., and D. S. Zrnić, 1990a: Estimation of rain and hail rates in mixed-phase precipitation. *J. Atmos. Sci.*, **47**, 565–683.
- \_\_\_\_\_, and \_\_\_\_\_, 1990b: Use of polarization to characterize precipitation and discriminate large hail. *J. Atmos. Sci.*, **47**, 1525–1540.
- Battan, L. J., 1973: *Radar Observation of the Atmosphere*, University of Chicago Press, 324 pp.
- Brandes, E. A., and J. Vivekanandan: 1998: An exploratory study in hail detection with polarimetric radar. *Preprints*, 14<sup>th</sup> International Conference on Interactive Information and Processing Systems for Meteorology, Oceanography, and Hydrology. Phoenix, Arizona, Amer. Meteor. Soc., 287–290.
- \_\_\_\_\_, G. Zhang, and J. Vivekanandan, 2002: Experiments in rainfall estimation with a polarimetric radar in a subtropical environment. *J. Appl. Meteor.*, **41**, 674–685.
- \_\_\_\_\_, \_\_\_\_\_, and \_\_\_\_\_, 2004: Drop size distribution retrieval with polarimetric radar: Model and application. *J. Appl. Meteor.*, **43**, 461–475.
- Bringi, V. N., T. A. Seliga, and K. Aydin, 1984: Hail detection with a differential reflectivity radar. *Science*, **225**, 1145–1147.
- Doviak, R., and D. Zrnić, 1993: *Doppler Radar and Weather Observations*, Academic Press, 562 pp.
- Goddard, J. W. F., J. Tan, and M. Thurai, 1994: Technique for calibration of meteorological radars using differential phase. *Electron. Lett.*, **30**, 166–167.
- Golestani, Y. V. Chandrasekar, and V. N. Bringi, 1989: Intercomparison of multiparameter radar measurements. *Preprints*, 24<sup>th</sup> Conf. on Radar Meteorology, Tallahassee, Florida, Amer. Meteor. Soc., 309–314.
- Green, A. W., 1975: An approximation for shapes of large drops. *J. Appl. Meteor.*, **14**, 1578–1583.
- Heinselman, P. L., and A. V. Ryzhkov, 2004: Hail detection during the Joint Polarization Experiment. *Preprints*, 22<sup>nd</sup> Conference on Severe Local Storms, Hyannis, Massachusetts, Amer. Meteor. Soc.
- Husson, D., and Y. Pointin, 1989: Quantitative estimation of the hailfall intensity with a dual polarization radar and a hailpad network. *Preprints*, 24<sup>th</sup> Conf. on Radar Meteorology, Tallahassee, Florida, Amer. Meteor. Soc., 318–321.
- Illingworth, A. J., J. W. F. Goddard, and S. M. Cherry, 1986: Detection of hail by dual-polarization radar. *Nature*, **320**, 431–433.
- Knight, C. A., and N. C. Knight, 1970: The falling behavior of hailstones. *J. Atmos. Sci.*, **27**, 672–681.
- Leitao, M. J., and P. A. Watson, 1984: Application of dual linearly polarized radar data to prediction of microwave path attenuation at 10–30 GHz. *Radio Sci.*, **19**, 209–221.
- Lipschutz, R. C., J. F. Pratte, and J. R. Smart, 1986: An operational  $Z_{DR}$ -based precipitation type/intensity product. *Preprints*, 23<sup>rd</sup> Conf. on Radar Meteorology, Snowmass, Colorado, Amer. Meteor. Soc., JP-91–JP-94.
- Nanni, S., P. Mezzasalma, and P. P. Alberoni, 2000: Detection of hail by polarimetric radar data and hailpads: Results from four storms. *Meteorol. Appl.*, **7**, 121–128.
- Ryzhkov, A. V., and D. S. Zrnić, 1994: Precipitation observed in Oklahoma mesoscale systems

- with polarimetric radar. *J. Appl. Meteor.*, **33**, 455–464.
- \_\_\_\_\_, and \_\_\_\_\_, 1998: Beamwidth effects on the differential phase measurements of rain. *J. Atmos. Oceanic Technol.*, **15**, 624–634.
- Seliga, T. A., and V. N. Bringi, 1976: Potential use of radar differential reflectivity measurements at orthogonal polarizations for measuring precipitation. *J. Appl. Meteor.*, **15**, 69–76.
- \_\_\_\_\_ and \_\_\_\_\_, 1978: Differential reflectivity and differential phase shift: Applications in radar meteorology. *Radio Sci.*, **13**, 271–275.
- Smyth, T. J., T. M. Blackman, and A. J. Illingworth, 1999: Observations of oblate hail using dual polarization radar and implications for hail-detection schemes. *Quart. J. Roy. Meteor. Soc.*, **125**, 993–1016.
- Ulbrich, C. W., and D. Atlas, 1982: Hail parameter relations: A comprehensive digest. *J. Appl. Meteor.*, **21**, 22–43.
- Vivekanandan, J., G. Zhang, S. M. Ellis, D. Rajopadhyaya, and S. K. Avery, 2003: Radar reflectivity calibration using differential propagation phase measurement. *Radio Sci.*, **38**, doi:10.1029/2002RS002676.
- \_\_\_\_\_, D. S. Zrníc, S. M. Ellis, R. Oye, A. V. Ryzhkov, and J. Straka, 1999: Cloud microphysics retrieval using S-band dual-polarization measurements. *Bull. Amer. Meteor. Soc.*, **80**, 381–388.
- Zhang, G., J. Vivekanandan, and E. Brandes, 2001: A method for estimating rain rate and drop size distribution from polarimetric radar measurements. *IEEE Trans. Geosci. Remote Sens.*, **39**, 830–841.
- Zrníc, D. S., V. N. Bringi, N. Balakrishnan, K. Aydin, V. Chandrasekar, and J. Hubbert, 1993: Polarimetric measurements in a severe hailstorm. *Mon. Wea. Rev.*, **121**, 2223–2238.